ATLAS Internal Note
TILECAL-NO-054
16 August 1995

Calculation of the Atlas magnetic field

F. Bergsma / PPE-EC
CERN, Geneva, Switzerland
August 1995

Fig. 1

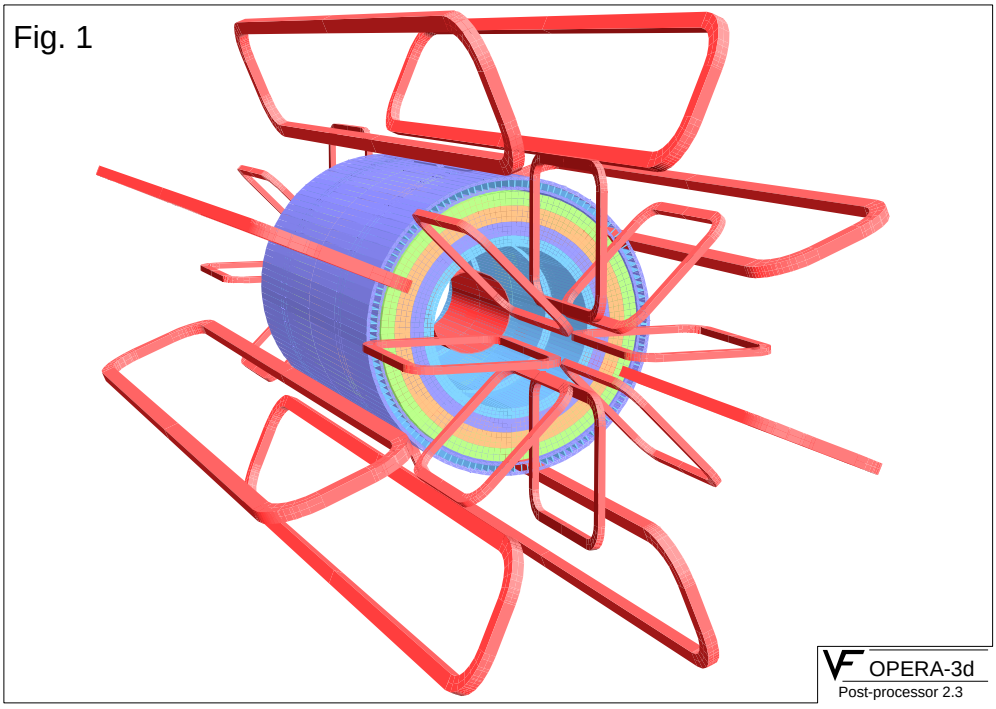

Abstract

A magnetic fieldmap of the complete ATLAS detector was made using the FEM-program TOSCA. The model includes all coils and magnetizable components. Only 1/16th of the total space was meshed, applying symmetry. The tile calorimeter was emulated with homogeneous anisotropic material. The results and all details about the model are contained in the database atlx16l.toscab in directory /afs/cern.ch/user/b/bergsma/public, where some command files to exploit the database and a user guide can be found.

1 Introduction

An attempt was made to model the complete ATLAS detector, including all coils and magnetizable components. Since solenoidal and toroidal coils have different symmetry properties, a model that contains both is necessarily larger than a model that contains only one of them.
A difficult object for calculation is the tile calorimeter, which is build from many small parts. In order to keep the size of the model within limits, the tilecal was emulated with homogeneous anisotropic material, of which the permeability was made equal to the mean permeability of the real tiles.
The FEM-program TOSCA from Vector Fields [1] was used.

2 The model

Fig. 1 shows the main magnetizing and magnetizable components of the Atlas detector: solenoid, barrel toroid, forward toroids and the tile calorimeter with its support bars. For clarity in this figure some shielding plates and the inner forward toroid coils were left out.
It is assumed that the beam-axes is the z-axes, the x-axes is horizontal and the y-axes vertical. The origin is in the center of the detector. Some dimensions are given in appendix A, all dimensions can be found in the database.

2.1 The mesh

In fig. 1 one can see that every rotation of 45 degrees around the beam-axes maps the detector onto itself, with conservation of current direction. This makes it possible to mesh only 1/8th of the total problem space.
A rotation of 180 deg. around an axes through the center of the detector, perpendicular to the beam-axes and crossing a barrel or forward toroid coil (i.e. an axes formed by rotation of n x 22.5 deg. of the x-axes around the z-axes) maps the detector also back onto itself, but with current direction inverted in toroids and solenoid. This makes it possible to reduce the mesh to 1/16th of the total problem space.
The area to be meshed is indicated in fig. 2 . It is one halve of a 45 deg. segment of the z-axes, limited by two barrel or forward toroid coil planes.

Fig. 2

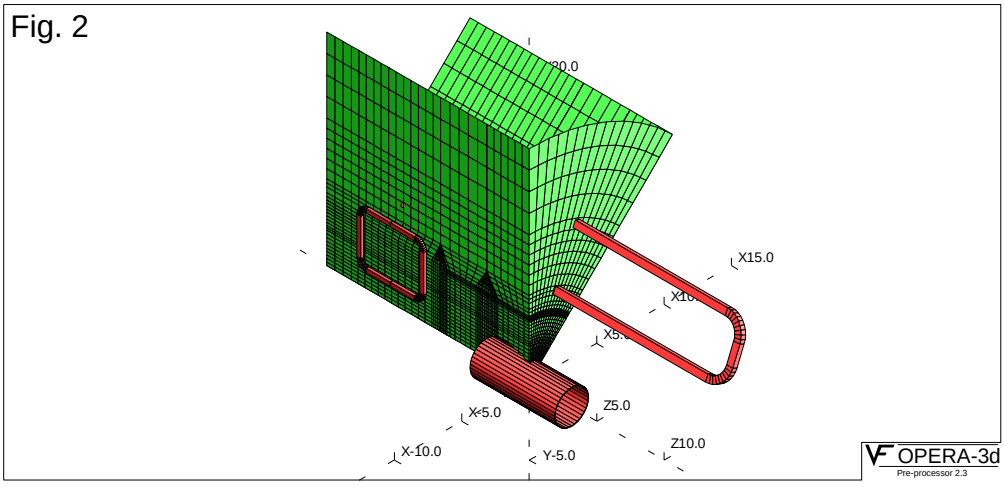

A further reduction is not possible, the solenoid and toroid spoil each other's symmetry. Without toroids the problem would reduce to a two-dimensional one due to cylindrical symmetry, with another 4-fold symmetry due to reflection about the z- and r-axes. Without solenoid the area of fig.2 could be halved by reflection relative to a toroid coil plane, giving a reduction of 1/32. However by this reflection the solenoid current would change direction, whereas the toroid current would remain unchanged. Due to the non-linear permeability of the iron the toroid and solenoid fields can not be separated and one has to model 1/16 of the total problem space (see also fig.5).

2.2 Boundary conditions

The planes limiting the meshed area given in fig. 2 obtain the boundary condition “symmetry” (see [1]). The potential on each point of a side plane will be the same as the potential on the corresponding point of the other side plane, obtained by a 45 deg. rotation around the z-axes. This will be called transformation 1.
The potential of each point in the front plane is made equal to the negative potential of the corresponding point in the front plane, obtained by a 180 deg. rotation around an axes in that plane, making an angle of 22.5 deg. with the y-axes. This will be called transformation 2.
The points on the cross-lines of the symmetry planes in fig.2 get a potential of zero, since due to transformation 1: pot1=pot2 and due to transformation 2: pot1=-pot2 => pot1=pot2=0. The points on the rotation axes get also pot=0. Since it seems only possible in Tosca to set facets to a certain potential value, a thin layer was created at z=0 in the x,y-plane, with extruded facets set to pot=0. By a point transformation the boundary facets of this layer were reduced to a line. The rotation axes gets the value of pot=0 set by the program. In the top and back planes of the segment of fig.2,which are not drawn, the normal component of the field is set to zero.

2.3 Materials

In fig.3 a 1/256 segment of the detector is shown. From this a 1/16 segment can be created by 1 x reflection and 8 x rotation over 5.625 degrees. The BH-curve used for all solid iron parts is given in appendix C. For the permeability of the tilecal see section 2.5.
All air around the tilecal is made reduced potential area. The space inside the cylinder formed by the support bars of the tilecal is set to total potential, except for an inner cylinder around the solenoid.

Fig. 3

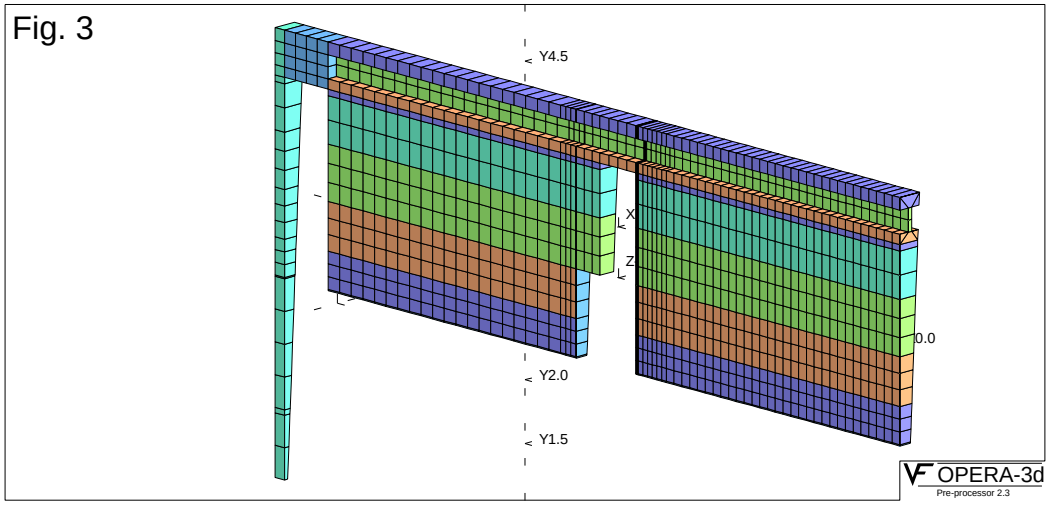

2.4 Coils

The current in the solenoid is 9.30 MAmp, in the barrel toroid 3.04 MAmp per coil. In the forward toroids currents of 0.4 Mamp in the inner coils and 1.52 Mamp in the outer coil were applied. The Tosca conductor file is given in appendix B.

2.5 Tilecal

In fig.4 a piece of a tilecal segment is shown. One segment covers 360/64 deg., has a radial length of 1.57 m and a length of 0.36 m in the z-direction. It is made out of solid iron plates of 5 mm thickness, glued together with 4 mm thick iron spacers. In the holes between the spacers scintillators will be placed. The glue layer between plates and spacers has an estimated thickness of 0.05 mm.
Although very small, this glue layer will change the permeability in the direction perpendicular to the plates drastically. This is easy to understand, if one realizes that in the absence of a glue layer the magnetic flux will pass through a bottleneck of a few mm length, formed by the plate and two neighboring spacers on each side of the plate. The glue layers between these spacers take of the order of

two percent of this length, reducing its relative permeability of about 5000 for typical magnetic steel to about 1/(0.02)=50.
Since there was not enough computing power available to include the complete tile calorimeter in the model, the tiles were treated as a homogeneous anisotropic material.
If one defines $\overline{B} = \int_{tile} B dv / Vtile$ and $\overline{H} = \int_{tile} H dv / Vtile$, with Vtile the volume of the smallest block from which the full tile structure can be build, one has

$$\text{div } B = 0 \rightarrow \text{div } \overline{B} = 0 \quad \text{rot } H = J \rightarrow \text{rot } \overline{H} = \overline{J}$$

and B can be replaced by $\overline{B}$, H by $\overline{H}$ in a model of the full detector to calculate the magnetic field, without using the tile structure in detail.
The relation between $\overline{B}$ and $\overline{H}$ is calculated in the section below on a small test cell with complete tile structure. This method implies that the rate of change of the boundary conditions is small over the tile dimension.
Once $\overline{B}$ and $\overline{H}$ are calculated one can obtain the local field from (7)-(9) of the next section. This is of particular importance for track reconstruction.

Fig. 4

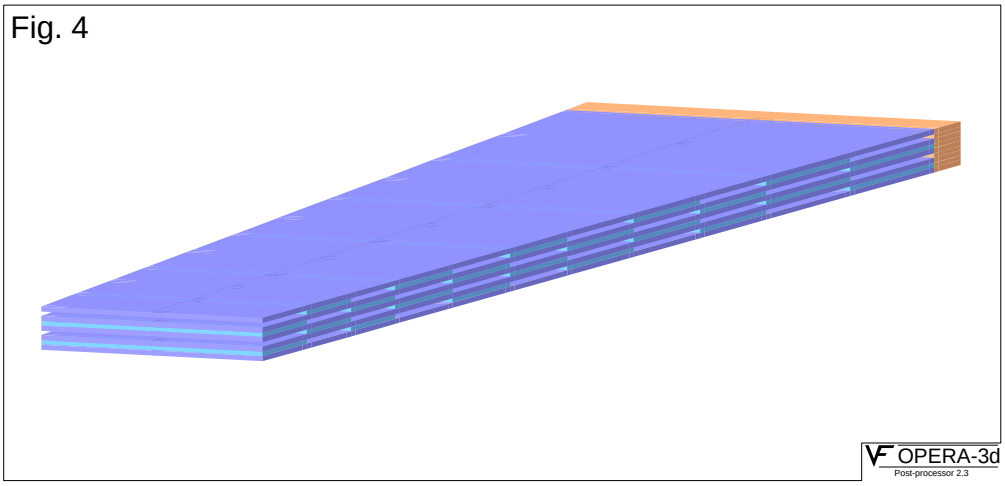

2.5.1 analytical calculation of mean permeability

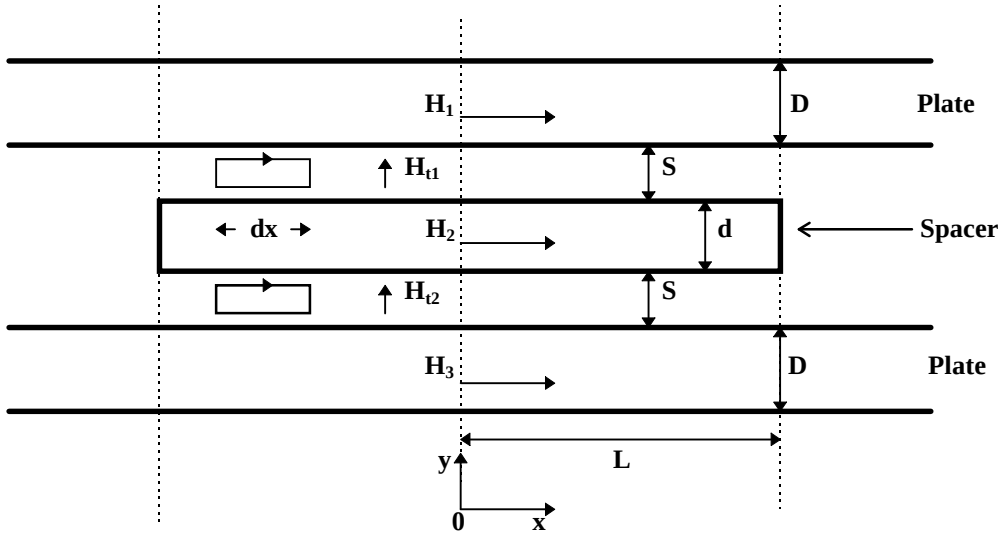

In the figure above a minimal segment is shown of which the tilecal can be constructed by displacement over a length n x 2L in the x-direction and m x (D+d+2S) in the y-dir.
It is assumed that the flux in plates and spacers is uniformly distributed in the x-direction, i.e. $d,D/\mu << S \Rightarrow Hy \approx 0$ in plates and spacers.
Considering the field over a length dx one has:

$\nabla x\, H = 0 \Rightarrow$

$$\frac{dH_{t1}}{dx} = (H_1 - H_2)/s \tag{1}$$

$$\frac{dH_{t2}}{dx} = (H_2 - H_3)/s \tag{2}$$

$\nabla . B = 0 \Rightarrow$

$$\frac{d\mu_1 H_1}{dx} = \frac{\mu_0}{D} H_{t1} \tag{3}$$

$$\frac{d\mu_3 H_3}{dx} = -\frac{\mu_0}{D} H_{t2} \tag{4}$$

$$\frac{d\mu_2 H_2}{dx} = -\frac{\mu_0}{d} H_{t1} + \frac{\mu_0}{d} H_{t2} \tag{5}$$

If μ=constant, (1)-(5) is a system of linear differential equations of first order. Together with the symmetry boundary conditions

$$\begin{aligned} H_1(x) &= H_3(-x) \\ H_2(x) &= H_2(-x) \\ H_{t1}(x) &= H_{t2}(-x) \end{aligned} \tag{6}$$

it has the following solution

$$H_{1,3} = \pm\Delta\frac{\sinh(\lambda_1 x)}{\sinh(\lambda_1 L)} + \frac{1}{2}\left(\frac{d}{D}\frac{\cosh(\lambda_2 x)}{\cosh(\lambda_2 L)} + 1\right)\frac{T}{\mu(2D+d)} \tag{7}$$

$$H_2 = \left(1 - \frac{\cosh(\lambda_2 x)}{\cosh(\lambda_2 L)}\right)\frac{T}{\mu(2D+d)} \tag{8}$$

$$H_{t1,2} = \mu_r D\Delta\lambda_1\frac{\cosh(\lambda_1 x)}{\sinh(\lambda_1 L)} \pm \frac{1}{2}\frac{d\cdot T}{\mu_0(2D+d)}\lambda_2\frac{\sinh(\lambda_2 x)}{\cosh(\lambda_2 L)} \tag{9}$$

$$\lambda_1 = \sqrt{\frac{1}{\mu_r DS}}$$

$$\lambda_2 = \sqrt{\frac{1}{\mu_r S}\left(\frac{2}{d} + \frac{1}{D}\right)}$$

$$T = \mu DH_1 + \mu DH_3 + \mu dH_2 =$$

= flux in x-direction

$$\Delta = \frac{\pm(H_1 - H_3)_{x=\mp L}}{2}$$

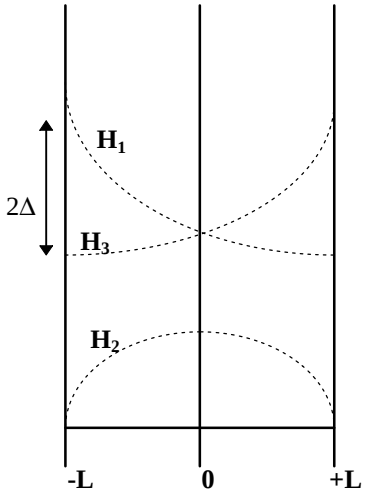

From the preceding equations one can derive:

$$\overline{\mu_x} = \frac{\overline{B_x}}{\overline{H_x}} = \mu\left(1 - \frac{d+4S}{2(D+d+2S)}\right)\cdot\frac{1}{\frac{\sinh(\lambda_2 L)}{2\lambda_2 L\cosh(\lambda_2 L)}\cdot\frac{d}{D} + 1} \tag{10}$$

$$\overline{\mu_y} = \frac{\overline{B_y}}{\overline{H_y}} = \frac{1}{2}\mu_0\left(\frac{D+d+2S}{2S}\right)\cdot\frac{\sinh(\lambda_1 L)}{\lambda_1 L\cosh(\lambda_1 L)} \tag{11}$$

$$+\mu_0\left(\frac{D+d+2S}{2S}\right)\cdot\left(2 - \frac{\sinh(\lambda_1 L)}{\lambda_1 L\cosh(\lambda_1 L)}\right)$$

$$\overline{\mu_z} = \lim_{L\to\infty}\overline{\mu_x} = \mu\left(1 - \frac{d+4S}{2(D+d+2S)}\right) \tag{12}$$

$$\frac{\overline{B_{y\,\mathrm{scint}}}}{\overline{B_y}} = \frac{2\cosh(\lambda_1 L) - \cosh(\lambda_1 x)}{\left(\frac{d+2S}{4S} - 1\right)\frac{\sinh(\lambda_1 L)}{\lambda_1 L} + 2\cosh(\lambda_1 L)} \tag{13}$$

2.5.2 discussion of results

As a check on the correctness of (10)-(13) it is mentioned that they all give the right limit if μ or L approaches infinity.
For decent values of μ, S and L the sinh and cosh terms in (11) are almost equal, which means μ_y is about proportional to sqrt(μ_r/S). So even though rather big fluctuations are to be expected in the values of μ_r and S, their influence on μ_y will be reduced. In addition the global field will be determined by a value of μ_y averaged over many plates. However, the precision of the model described above should be determined by measurement.
A tilecal segment can be placed inside a magnet and the ratio of the field inside the scintillator gaps over the field on the surface of the segment can be measured and compared with (13). Some preliminary measurements were done by placing the subsegment shown in fig. 4 in an H-magnet with 2 x 0.56 m2 flat poles and a gap width of 0.2 m. Calculation showed that the flux on the surface not too far away from the edges is a good measure for the average flux in the segment and measurements were compatible with (13). More measurements are needed and the BH-curve of the plates and spacers has to be determined.

2.5.3 Tilecal permeability used in the model

The BH-curve used for the solid iron parts of the detector is shown in appendix C. As one can see for field values up to 0.64 Tesla it yields a constant μ_r of 6400. This value is used, together with S=0.05 mm, D=5 mm, d=4 mm in (10)-(12) to give:

2L	**100**	**130**	**150**	**190**
μ_x	**0.66** μ_{Fe}	**0.68** μ_{Fe}	**0.69** μ_{Fe}	**0.71** μ_{Fe}
μ_y	**34** μ_0	**29** μ_0	**26** μ_0	**22** μ_0
μ_z	**0.77** μ_{Fe}	**0.77** μ_{Fe}	**0.77** μ_{Fe}	**0.77** μ_{Fe}

It is mentioned that in the case of infinitely high μ of the iron and the same values of D, d and S, μ_y would be 45.5 μ_0.
Unfortunately one has not the freedom in Tosca to set $\mu_{x,y,z}$ for each element as function of $H_{x,y,z}$. An approximation was chosen, using the laminated material option of Tosca (see [1]). One single BH-curve of 0.77 μ_{Fe} was assigned to the tilecal and the packing factor was set to get the right value of μ_y. This gives the following values: (pack=1-1/μ_y μ_x=μ_y=pack*0.77). Like this one obtains the right value for μ_y and $\approx$10% deviations for $\mu_{x,z}$.
These values were used as a first approximation in the regions shown in fig. 3. The effect of the deviations in μ_x and μ_y on the field in the tilecal is small. The field in most places of the tilecal is so low that the iron is far away from saturation and the application of a constant μ justified.
It is possible to make a more precise calculation of the tilecal permeability, by allowing variations in μ in the integration of (1)-(5). Probably the manufacturer of Tosca is willing to implement some extensions to the permeability assignment of the elements. Before it is worth to carry out such an effort more measurements on tile-modules should be performed.

3 Results

The calculation took approx. 7.5 hours of CPU-time on the CERN IBM RS6000 (PARC) cluster. The model has 97481 nodes, currently the maximum amount of nodes on PARC is set to 100000. The result is contained in the database atlx16l.toscab on /afs/cern.ch/user/b/bergsma/public. In the same directory one can find some command files to exploit the database and some explanation. In appendix D a command file is shown, which calculates the field at the points specified in an inputfile and puts the result in an output file.
In fig. 5 a contourplot of the field in a plane perpendicular to the z-axis at 2 m distance from the center is displayed. The solenoid and two barrel toroid coils are visible. The tilecal runs from y=2.3 to y=3.8, beyond the support bar starts. The fact that not all PM-cavities are visible and that the end plate seems to be too thick is caused by the resolution of the grid used to make this picture, the local mesh has a finer graduation. In this picture the interval between two contourlines is 400 gauss, the smallest closed

contour inside the tilecal (#2) is one of 400 gauss. One can see how the return flux from the support bar towards the solenoid causes an asymmetry with the toroid flux with respect to the plane through the solenoid coil. The unsmoothness of the contourlines inside the tilecal show the limited resolution of the used meshing and is an indication for the precision.
The return flux from the solenoid at z=0 is distributed as follows:

support bar	78.6 %
tilecal	13.0 %
endplate	1.9 %
air between solenoid and tilecal	3.3 %
missing	3.2 %

The amount of missing flux is an indication for the overall precision of this calculation.
The magnetic field inside the PM-cavities is everywhere below 20 gauss.
Using (13) it is found that the field inside the scintillators of the tilecal is below 40 gauss, except for a small region at the edges of the crack region.
For the determination of the precision of this model more studies are necessary. For the moment only a conservative limit can be given of 5% relative error in all regions except for the tile calorimeter and close to sharp edges. For the tilecal a relative error of 20% should be applied. In reduced potential areas the error should be applied only to the field caused by magnetized iron.

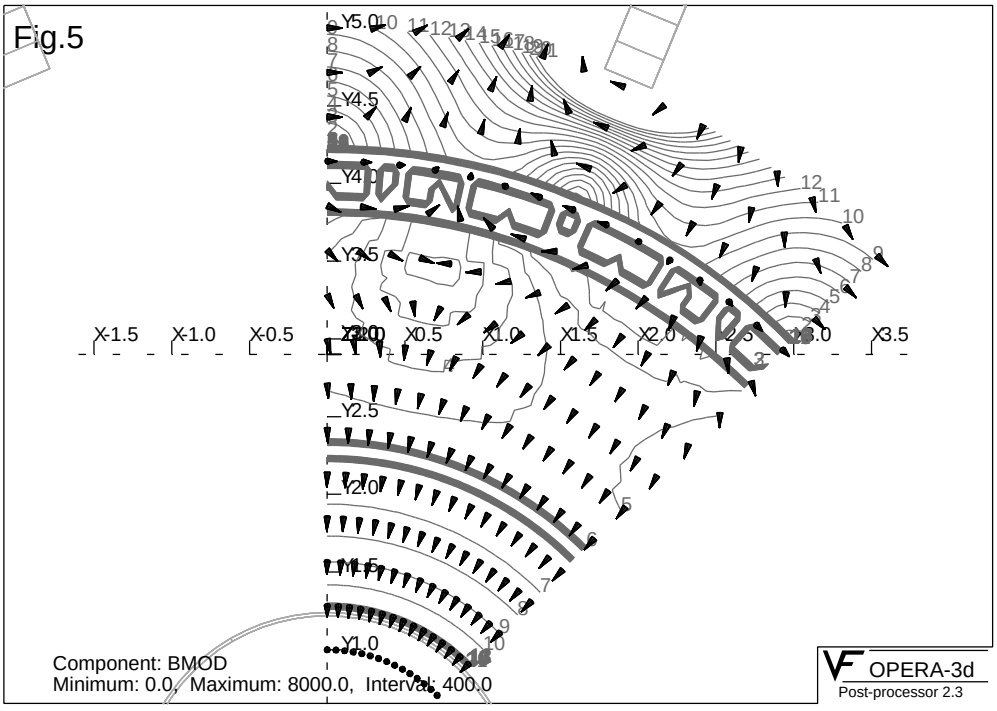

4 Next

The precision of the model should be determined with higher accuracy and improved. The improvement can be achieved by optimization of the model and by a more precise determination of its input parameters.
It is possible to optimize the grid, e.g. a progressive azimuthal refinement with increasing radius. On several places one can still economize on the node density. The current model has 10^5 nodes, it seems possible without to much trouble to increase the node limit to 3.10^5.
A precise measurement of the BH-curves of the iron of support bars and tilecal is necessary. Testing of tilecal segments should be continued to determine the mean value and standard deviation of the thickness of the glue layer between plates and spacers. With a slight modification of the Tosca code it

would be possible to use a non-diagonal BH-matrix, however for this the help of the manufacturer is necessary.

Reference

[1] Opera-3d reference manual, Vector Fields Limited, 24 Bankside, Kidlington, Oxford OX5 1JE, England

Appendix A Dimensions

all lengths in m

Support bars:

thickness outer layer: 0.100
thickness inner layer: 0.081
radial walls: 0.19 x 0.035
rmin, rmax : 3.860 , 4.230
length in beam dir: 12.200

Tile calorimeter:

end plate thickness: 0.010
length barrel tilecal in z-direction: 5.638
length extended barrel tilecal in z-direction: 2.650
gap size between barrel and ext. barrel tilecal: 0.631
rmin, rmax tilecal: 2.290 3.860

Barrel toroid:

8 x conductor 0.437 x 0.329
inner cond at 5.279 from beam axes
outer cond at 9.121 from beam axes
length in z-direction 24.955
radii of bent parts 1.016
current 8 x 3.04 MAmp

Forward toroids:

center at 10.200 from detector center
inner cond of outer coil at 1.043 from beam axes
outer cond of outer coil at 4.867 from beam axes
current outer coil 8 x 1.520 Mamp
current inner coils 8 x 0.400 MAmp

Solenoid:

length 5.300
inner radius 1.218
outer radius 1.240
current 9.299 MAmp

Appendix B Tosca conductor file

```
COND
DEFI GRAC
0.0         0.0         0.0         22.5
0.0         7.2         0.0
0.0         90.0        0.0
0.43718     0.32863
1.7029      -0.16432
11.2431     1.01577
2115.96         8 0.0
   0     0     0
10.0
DEFI GSOL
0.0         0.0         0.0         0.0
0.0         0.0         0.0
90.0        90.0        90.0
1.218       2.65        1.218       -2.65
1.24        -2.65       1.24        2.65
0.0         0.0         0.0         0.0
7975.0          1 0.0
   0     0     0
10.0
DEFI GRAC
0.0         0.0         0.0         0.0
0.0         3.87075     -10.2
0.0         90.0        0.0
0.075       0.19
0.55325     -0.095
1.33675     0.55325
2807.0          8 0.0
   0     0     0
10.0
DEFI GRAC
0.0         0.0         0.0         0.0
0.0         3.42283     -10.2
0.0         90.0        0.0
0.075       0.19
1.14575     -0.095
1.33675     0.70325
2807.0          8 0.0
   0     0     0
10.0
DEFI GRAC
0.0         0.0         0.0         0.0
0.0         3.20575     -10.2
0.0         90.0        0.0
0.075       0.19
1.44325     -0.095
1.715       0.4
2807.0          8 0.0
   0     0     0
10.0
DEFI GRAC
0.0         0.0         0.0         0.0
0.0         2.9545      -10.2
0.0         90.0        0.0
0.285       0.19
1.7695      -0.095
1.715       0.475
2807.0          8 0.0
   0     0     0
10.0
QUIT
```

Appendix C BH-curve

29 1 1
0.0000000E+00 0.0000000E+00
0.6400000E+00 0.7957747E+02
0.9200000E+00 0.1352817E+03
0.1009999E+01 0.1591550E+03
0.1099999E+01 0.1909859E+03
0.1200000E+01 0.2387324E+03
0.1299999E+01 0.3183098E+03
0.1400000E+01 0.4933801E+03
0.1450000E+01 0.6445774E+03
0.1500000E+01 0.8753523E+03
0.1549999E+01 0.1273240E+04
0.1575000E+01 0.1591550E+04
0.1599999E+01 0.2148592E+04
0.1650000E+01 0.3342254E+04
0.1700000E+01 0.4774648E+04
0.1750000E+01 0.6525352E+04
0.1799999E+01 0.9151410E+04
0.1849999E+01 0.1193662E+05
0.1900000E+01 0.1511972E+05
0.1950000E+01 0.1854155E+05
0.2000000E+01 0.2228169E+05
0.2049999E+01 0.2745423E+05
0.2099999E+01 0.3580986E+05
0.2150000E+01 0.4774649E+05
0.2200000E+01 0.6366198E+05
0.2250000E+01 0.9390137E+05
0.2299999E+01 0.1273239E+06
0.2928317E+01 0.6273239E+06
1.0000000E+01 6.2547904E+06

Appendix D Command file

Command file (atlx16l.comi) :

```
dummy
16
$cominput mode=continuous
UNIT METR
acti atlx16l.toscab
 LOAD
SET FIEL=NODA coil=inte
 table infi=input.table outf=atl1.table f4=bx f5=by f6=bz f7=bmod
end
```

Input file (input.table) :

```
   X       Y       Z         [METRE]
  .0     4.83     .0
 .65     4.83     .0
1.30     4.83     0
   0     4.83    -6.00
 .65     4.83    -6.00
1.30     4.83    -6.00
   0     7.36     0
1.00     7.36     0
2.00     7.36     0
   0     7.36    -9.00
```

Output file (atl1.table) :

X	Y	Z	BX	BY	BZ	BM [METRE]
.00000E+00	4.8300	.00000E+00	2706.3	.10805	-4.3333	2706.3
.65000	4.8300	.00000E+00	3070.0	2619.1	-4.2922	4035.4
1.3000	4.8300	.00000E+00	3417.5	6792.6	-3.6076	7603.9
.00000E+00	4.8300	-6.0000	2670.6	-37.517	10.900	2670.9
.65000	4.8300	-6.0000	3046.4	2565.0	49.157	3982.8
1.3000	4.8300	-6.0000	3426.5	6737.8	47.887	7559.2
.00000E+00	7.3600	.00000E+00	5152.9	.43672E-02	8.7180	5152.9
1.0000	7.3600	.00000E+00	5509.6	-1304.5	8.8159	5662.0
2.0000	7.3600	.00000E+00	6497.6	-3115.8	9.1669	7206.0
.00000E+00	7.3600	-9.0000	4920.7	-9.3912	17.530	4920.8